Diversification of *B. subtilis* during experimental evolution on *A. thaliana* and the complementarity in root colonization of evolved subpopulations

Christopher Blake[1], Mathilde Nordgaard[1], Gergely Maróti[2], Ákos T. Kovács[1,*]

[1] Bacterial Interactions and Evolution Group, DTU Bioengineering, Technical University of Denmark, 2800 Kongens Lyngby, Denmark

[2] Institute of Plant Biology, Biological Research Centre of the Hungarian Academy of Sciences, 6726 Szeged, Hungary

*For correspondence. E-mail: atkovacs@dtu.dk; Søltofts Plads Building 221, 2800 Kgs Lyngby, Denmark, Tel. +45 4525 2527; Fax +45 4588 4922

Keywords: *Bacillus subtilis*; experimental evolution; root colonization; biofilm; motility; morphotype

Summary

The soil bacterium *Bacillus subtilis* is known to suppress pathogens as well as promote plant growth. However, in order to fully exploit the potential as natural fertilizer, we need a better understanding of the interactions between *B. subtilis* and plants. Here, *B. subtilis* was examined for root colonization through experimental evolution on *Arabidopsis thaliana*. The populations evolved rapidly, improved in root colonization and diversified into three distinct morphotypes. In order to better understand the adaptation that had taken place, single evolved isolates from the final transfer were randomly selected for further characterization, revealing changes in growth and pellicle formation in medium supplemented with plant polysaccharides. Intriguingly, certain evolved isolates showed improved root colonization only on the plant species they evolved on, but not on another plant species, namely tomato, suggesting *A. thaliana* specific adaption paths. Finally, the mix performed better than the sum of its constituents in monoculture, which was demonstrated to be caused by complementarity effects. Our results suggest, that genetic diversification occurs in an ecological relevant setting on plant roots and proves to be a stable strategy for root colonization.

Significance Statement

Understanding how plant-growth-promoting rhizobacteria (PGPR) colonize plant roots is crucial to fully utilize their potential for agricultural applications. Here, we employ experimental evolution of the PGPR *Bacillus subtilis* on *Arabidopsis thaliana* to study root colonization. We revealed that evolving populations rapidly improve in root colonization and diversify into distinct morphotypes. Notably, improved root colonization by evolved isolates was observed on *A. thaliana*, not on tomato. Moreover, isolates of distinct morphotypes interacted during root colonization and the mixture of morphotypes showed higher productivity than predicted. These findings suggest that genetic diversification might be a stable strategy to maximize root colonization.

40 **Introduction**

41 The interplay between root-associated microbial communities and the plant itself is essential for the
42 productivity and health of the plant (Vandenkoornhuyse *et al.,* 2015). In general, these microbial
43 communities are highly diverse and comprise various complex interactions, both beneficial as well as
44 deleterious (Trivedi *et al.,* 2020). The plant host species tends to be one of the main drivers of variation
45 in the composition of the plant root microbiome, indicating an active selection of microbes by the
46 plant (Micallef *et al.,* 2009; Fitzpatrick *et al.,* 2018). Especially beneficial microbes, e.g. plant growth
47 promoting rhizobacteria (PGPR), are suggested to be actively recruited from the surrounding bulk soil
48 (Yi *et al.,* 2011; Pieterse *et al.,* 2014).

49 One widely studied PGPR is the Gram-positive, non-pathogenic, spore-forming bacterium *Bacillus*
50 *subtilis* (Cazorla *et al.,* 2007; Todorova & Kozhuharova, 2010; Luo *et al.,* 2015). *B. subtilis* is commonly
51 found in soil and has been isolated from various plant species (Cazorla *et al.,* 2007). It is widely
52 recognized to aid plants through multiple direct as well as indirect manners (Blake *et al.,* 2021). *B.*
53 *subtilis* is known to promote plant growth either through production of phytohormones or by
54 improving nutrient availability (Arkhipova *et al.,* 2005; Saravanakumar *et al.,* 2011; Sivasakthi *et al.,*
55 2014). In addition, *B. subtilis* protects the plant against pathogens, either directly by competing for
56 space and nutrients and by producing antimicrobials, or indirectly by triggering induced systemic
57 resistance (Lugtenberg & Kamilova, 2009; Pieterse *et al.,* 2014). One of the main mechanisms of plants
58 to attract and select for *B. subtilis,* is the secretion of root exudates, which act as chemoattractant and
59 nutrient source for microbes (Zhang *et al.,* 2014). Subsequently, *B. subtilis* needs to evade the innate
60 immune response of the plant and tightly attach to the root, often in the form of biofilms, providing
61 further opportunities for co-evolution with their host plant (Chen *et al.,* 2013; Deng *et al.,* 2019). Even
62 though some *B. subtilis* strains are already applied as biocontrol agents within agriculture, its success
63 under field conditions varies immensely (Peng *et al.,* 2011; Wei *et al.,* 2016). The main cause of this
64 variation, has been suggested to be the inability of *B. subtilis* to colonize and persist in the rhizosphere
65 for longer periods of time (Shoda, 2000).

66 Up until now, most studies analyzing the importance of bacterial properties for successful root
67 colonization by *B. subtilis* used either constructed mutant strains or distinct natural isolates
68 (Beauregard *et al.,* 2013; Chen *et al.,* 2013; Allard-Massicotte *et al.,* 2016; Dragoš *et al.,* 2018a;
69 Nordgaard *et al.,* 2021). This revealed, amongst other things, that the capability of *B. subtilis* to
70 colonize plant roots is tightly linked to its chemotactic response towards root exudates, as well as its
71 ability to form biofilms (Beauregard *et al.,* 2013; Chen *et al.,* 2013; Allard-Massicotte *et al.,* 2016).
72 Indeed, *B. subtilis* strains exhibiting strong pellicle formation - a type of biofilm formed at the liquid-
73 air interface – have been observed to show enhanced root colonization, while weak pellicle forming
74 strains showed reduced root colonization (Chen *et al.,* 2013). Biofilms consist of cells, that are packed
75 tightly together, embedded in a self-produced extracellular matrix (ECM), which for *B. subtilis* consists
76 mainly of an exopolysaccharide (EPS) and the protein TasA (Branda *et al.,* 2006; Arnaouteli *et al.,*
77 2021). Both, Beauregard *et al.* (2013) and Dragoš *et al.* (2018a) have shown that EPS and TasA are
78 required for successful root colonization, as mutants, Δ*eps* and Δ*tasA*, displayed a reduced number of
79 cells on plants, compared to the WT. On the contrary, inoculation of plant roots with a mixture of Δ*eps*
80 and Δ*tasA* led to a significantly higher root colonization compared to the WT, as matrix components
81 are shared and division of labor occurs between complementing Δ*eps* and Δ*tasA* mutants (Beauregard
82 *et al.*, 2013; Dragoš *et al.,* 2018a). Matrix components such as TasA and EPS are regarded as public
83 goods, i.e. compounds that are costly to produce but provide a collective benefit for the overall
84 population (Branda *et al.,* 2006; Zhang *et al.,* 2015; Dragoš *et al.,* 2018a). Public goods like matrix
85 components, however, not only provide the basis for division of labor, where resources are used and
86 shared efficiently, but might also allow exploitation, where cheaters are able to utilize the public good
87 without contributing to its production (van Gestel *et al.,* 2014; Dragoš *et al.,* 2018a, Dragoš *et al.,*
88 2018b).
89 Recently, a new study emerged using experimental evolution to analyze bacterial traits important for
90 plant microbial interactions (Batstone *et al.,* 2020). In general, experimental evolution might be less
91 constrained by preconceptions and is a powerful tool to analyze how microorganisms adapt to a wide

range of environments as well as to study evolutionary trade-offs (Kawecki *et al.,* 2012). By allowing cells to grow until the population reaches a high density, and subsequently transferring only a part of the population to new, fresh medium, continued growth is granted and therefore natural selection will drive the population over generations to adapt to the given conditions (McDonald, 2019). Batstone *et al.* (2020) used experimental evolution to evolve *Ensifer meliloti* on distinct *Medicago truncatula* genotypes in a greenhouse system in soil for five plant generations. *E. meliloti* rapidly adapted to its local host genotype, meaning that derived bacteria were both more beneficial and achieved higher fitness on the plant host genotype they shared an evolutionary history with (Batstone *et al.,* 2020).

In this study, we established a laboratory model system to inspect the evolution of *B. subtilis* on plant roots. 14-16d old *A. thaliana* seedlings were inoculated with *B. subtilis* in a minimal medium, after 2 days, the colonized root was subsequently transferred to fresh medium containing a new sterile seedling (14-16d old). This allowed us to follow evolving populations for 20 transfers and select for a regular root recolonization, including chemotaxis, biofilm formation and dispersal. We observed that evolving populations rapidly improved in root colonization and quickly diversified into distinct morphotypes. When these morphotypes were mixed together, they interacted on the root, and the mixed community showed “overyielding” compared to the predicted productivity. Intriguingly, even though variants with reduced biofilm formation ability displayed lessened root colonization in mono-culture, these were able to evolve and persist in most populations benefitting from the matrix overproduced by another morphotype. Finally, we observed increased root colonization of evolved isolates exclusively on *A. thaliana*. The lack of such increase on tomato (*Solanum lycopersicum*) roots suggested an *A. thaliana*-specific adaptation.

Results

B. subtilis shows rapid improvement and diversification during evolution on plant roots

117 To examine how the PGPR *B. subtilis* evolves on plant roots and adapts in root colonization, five
118 parallel populations (from A to E), started from a single clonal lineage of *B. subtilis* strain DK1042
119 (natural competent derivative of the undomesticated NCBI 3610 (Konkol *et al.,* 2013)), were passaged
120 on *A. thaliana* seedlings for 20 transfers, spanning over a total of 40 days (Fig. 1). To follow possible
121 improvements in root colonization during the experimental evolution, colony forming unit (CFU) per
122 gram of roots was assessed after transfer 1, 5, 10, 17 and 20 (T1, T5, T10, T17 and T20, respectively).
123 As expected, root colonization improved quickly in all evolving populations. The number of cells
124 colonizing the roots increased on average about 10-fold, considering all five populations, from the first
125 to the 5th transfer and stayed at similar level afterwards (Fig. 2A). Tukey´s test confirmed that T5, T10
126 and T20 were significantly different from T1, while T17 was not significantly different from any of the
127 others.

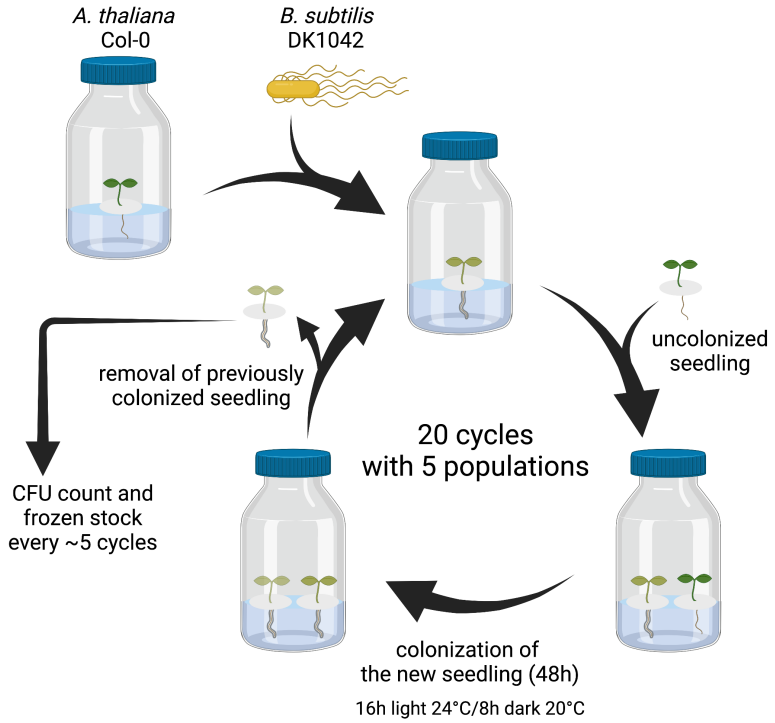

128

129 **Fig. 1.** Experimental evolution scheme of parallel populations of *B. subtilis* (see Experimental
130 procedures for detailed description of conditions used). Created with BioRender.com.
131

132 Furthermore, in all five populations, three very distinct morphological variants were observed in the
133 CFU assays. These include a Snow (SN) variant with hyper-wrinkled, whitish colony morphology, a

134 Smooth (SM) variant with round, smooth and shiny colony morphology and a Wrinkled (WR) variant
135 with a colony morphology identical to the ancestor (Fig. 2B). Because WR variants were
136 indistinguishable from the ancestor by sheer colony morphology, only cultures directly from the
137 ancestral stock were regarded and termed as ancestor in this report, while all other colonies and
138 cultures, i.e. those that were observed after the first transfer of experimental evolution, were counted
139 as WR. Importantly, identification of morphotypes via serial dilution plating on LB-agar has its
140 limitations in the range of detection, therefore, the presence of morphotypes in low abundances
141 under detectable levels cannot be excluded. Genetic stability of the three distinct morphotypes was
142 confirmed by repeated passaging on either solid medium, in liquid culture or alternating between the
143 two for a chosen representative example of each morphotype isolated from three populations
144 (population A, D, and E). SN was observed in all five populations at T5 reaching in average a final
145 frequency of around 20% (Fig. 2CD). SM was observed in all five populations at T10, except for
146 population E, where it was observed after T15. The final frequencies of the morphotypes were highly
147 similar across all five populations, except for population B, where SM was below detection level at T20
148 (Fig 2D).

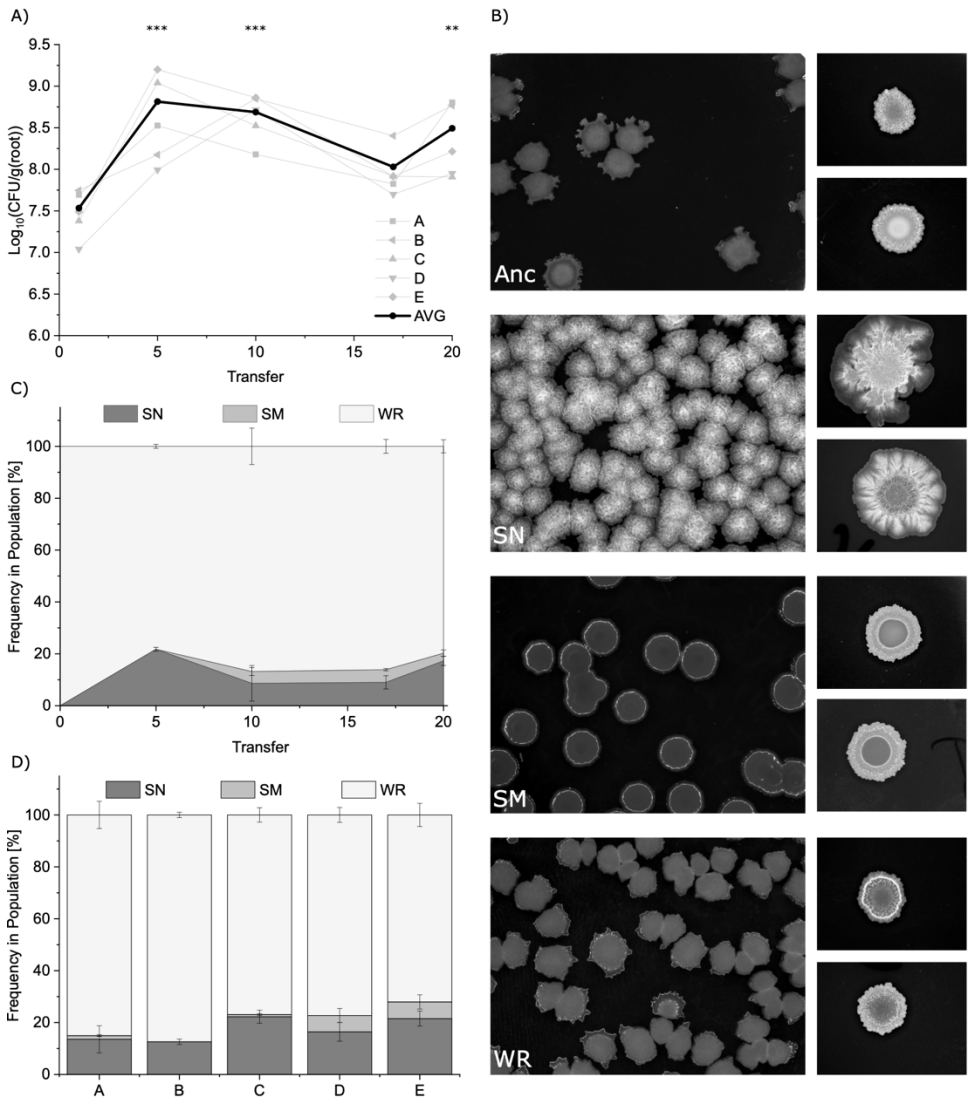

Fig. 2. Adaptation in root colonization and diversification of *B. subtilis* on *A. thaliana*. A. Changes in root colonization during experimental evolution was monitored as CFU per gram root for T1, T5, T10, T17 and T20 in populations A to E. (**: $p<0.01$, ***: $p<0.001$). B. Distinct colony morphologies were identified and described based on colony architecture when plated (left) or spotted (right, two representative samples) on 1.5% LB-Agar after 48h incubation at 30°C for the ancestral strain (Anc), snow morphotype (SN), smooth morphotype (SM) and wrinkled morphotype (WR). C. Relative frequencies of different morphotypes in subsequent evolutionary time points in average of all five populations (n=5). D. Final (T20) relative frequencies of different morphotypes in all five parallel evolved populations (n=3). For panel C and D, data represent mean and error bars represent standard error.

Pellicle formation and growth on plant polysaccharides correlate with distinct morphotypes

To further explore the phenotypic traits of the three distinct morphotypes, morphologically distinct isolates from the final transfer were randomly selected, and tested for growth and biofilm pellicle formation in response to plant polysaccharides. As *B. subtilis* was evolved in a minimal salt medium

165 (see Experimental procedures), bacterial cells were dependent on carbon sources provided by the
166 plant for their growth. We hypothesized, therefore, that evolved isolates could adapt to the
167 environment by improving the utilization of plant polysaccharides. Indeed, most evolved isolates
168 showed altered planktonic growth in MSNc + 0.5% xylan. Growth patterns correlated well with the
169 specific morphotypes, i.e. prolonged stationary phase/delayed decline of SN, and higher growth rate
170 as well as higher maximum optical density (OD) of SM compared to the ancestor (Fig. 3A). Notably,
171 xylan displays some absorbance at OD_{600}. Therefore, the initial drop in OD_{600} can be attributed to the
172 time span where cells break down xylan, reducing OD_{600} until bacterial growth is able to exceed
173 (Beauregard *et al.*, 2013).
174 Pellicle formation has been proven to be not only a great indicator for biofilm productivity in general,
175 but also to correlate with root colonization by *B. subtilis* strains (Chen *et al.,* 2013). Beauregard *et al.*
176 (2013) demonstrated that plant polysaccharides act as a signal for biofilm formation in *B. subtilis* via
177 kinases of the Spo0A pathway. Xylan has been observed to be one of the strongest biofilm inducer
178 plant polysaccharides (Beauregard *et al.*, 2013). Here, we tested pellicle formation in LB medium in
179 the presence of the plant polysaccharide xylan in 24-well plates. This allowed us to test the inductive
180 effects on biofilm formation of *B. subtilis* by xylan*,* while still providing enough nutrients for robust
181 pellicles. After incubating for 48h at 30°C, pellicle complexity and architecture of evolved isolates were
182 analyzed in comparison to the ancestral strain. As expected, pellicle formation by the evolved isolates
183 mostly correlated with morphological appearance of colonies on solidified LB medium (Fig. 3B). Similar
184 to their colony morphology, SN variants produced hyper-robust pellicles, indicating overproduction of
185 matrix components (Fig. 3B). On the contrary, SM variants were unable to form a stable pellicle, only
186 a thin film was observed on the liquid-air interface (Fig. 3B). Notably, no major changes between
187 pellicles formed by WR compared to the ancestral strain were observed (Fig. 3B).

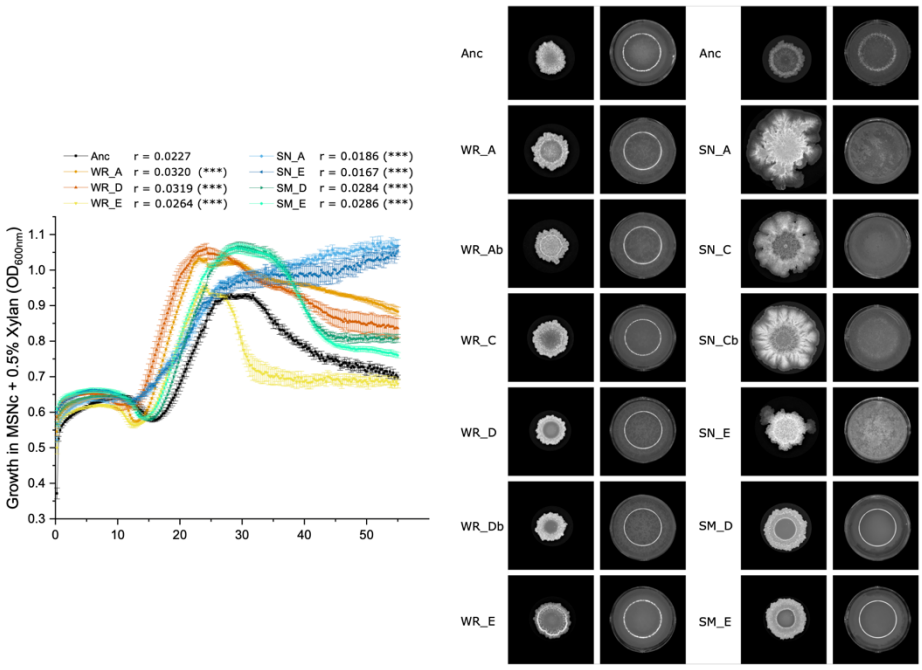

Fig. 3. Growth and pellicle formation of evolved isolates from final transfer (T20) in response to plant polysaccharides compared to the ancestor. A. Growth of evolved isolates and ancestor in MSNc + 0.5% xylan was followed at 24°C for 56h (n=6, 2 independent overnight cultures with each 3 replicates). Data represent mean and error bars represent standard error. Growth rates (r) have been calculated for exponential phase following a linear regression model (***: $p<0.001$). B. Colony and pellicle morphology developed by evolved isolates and ancestor. Colony morphology was tested by spotting 2µl of ON culture on 1.5% LB-Agar and incubating for 48h at 30°C. Pellicle morphology was studied by inoculating overnight cultures into 1 mL LB medium supplemented with 0.5% xylan at a starting OD_{600} of 0.075. Images of colonies and pellicle were obtained after 48h at 30°C.

Improvements in plant root colonization tend to be A. thaliana specific

Biofilm formation on the root by *B. subtilis* is initiated by the recognition of plant signals, and the composition of those signaling components is suggested to be plant species-specific (Warembourg *et al.,* 2003; Beauregard *et al.,* 2013). Therefore, we wondered whether improvements in root colonization might be specific and limited to the plant species they evolved on. To test this, we inoculated both 14-16d old *A. thaliana* seedlings as well as 6-8d old tomato seedlings with either our evolved isolates from the final transfer or with the ancestral strain and quantified plant colonization after 48h.

Intriguingly, we observed that 7 out of 12 isolates showed improved root colonization compared to the ancestral strain on *A. thaliana*, while none improved on tomato (Fig. 4). This indicates that, *B.*

209 *subtilis* adapted specifically to root colonization of *A. thaliana*. Interestingly, improvements in root
210 colonization tended to be only partially in accordance with the morphotypes of the tested isolates. All
211 four tested SN isolates, displayed improved root colonization on *A. thaliana*. This is consistent with
212 previous studies, which showed that enhanced biofilm formation leads to increased root colonization
213 (Chen *et al.,* 2013). On the contrary, WR and SM isolates showed varying results. Remarkably, only
214 SM_E showed reduced root colonization on both plant species in accordance with highly reduced
215 pellicle formation, while SM_D performed similar to the ancestor. Notably, the two SM isolates
216 evolved in distinct populations and might therefore harbor distinct mutations, therefore, additional
217 mutations in the two SM isolates could explain variation in root colonization.

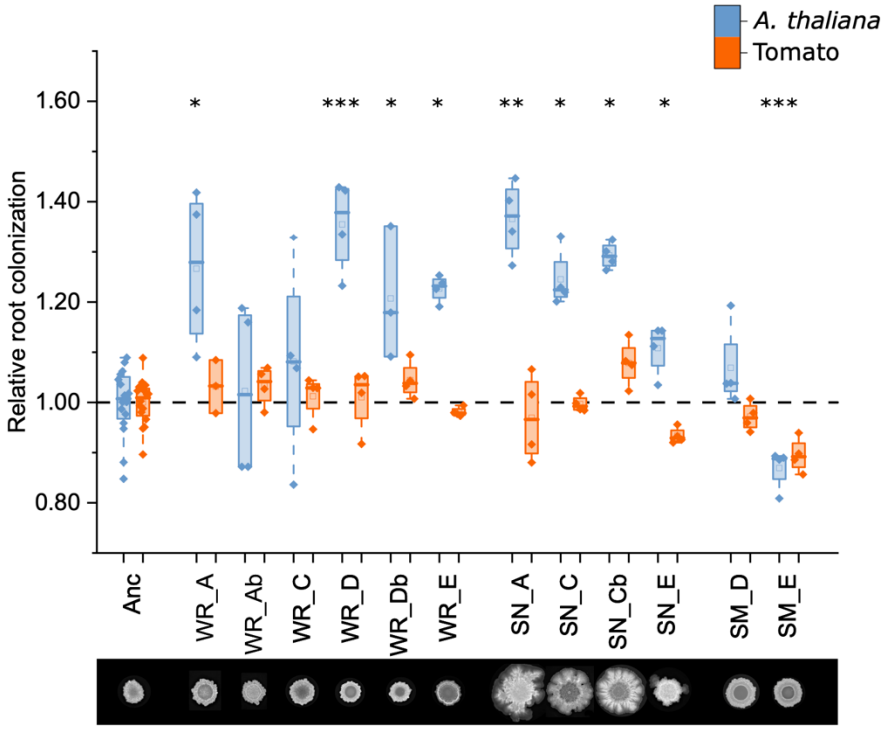

218

219 **Fig. 4.** Root colonization by evolved isolates from the final transfer (T20) compared to the ancestor.
220 Both 14-16 days old *A. thaliana* (blue) and 10-12 days old tomato seedlings (orange) were inoculated
221 with evolved isolates originating from different populations (populations A, C, D, and E) as well as the
222 ancestor and incubated for 48h in a plant chamber. The biofilm on the roots was disrupted through
223 vortexing with small glass beads and the suspension was plated on LB-agar medium to allow CFU
224 counting. For each isolate, relative root colonization was calculated by dividing the log10-transformed
225 CFU value of each replicate with the mean of the log10-transformed CFU of the ancestor from the
226 same experimental setup. Here, the pooled CFU of the ancestor from all experimental set-ups is
227 shown. The dashed line represents the mean of the ancestor. ANOVA followed by Post-hoc Dunnett´s
228 tests were performed to test for significance between each isolate and the ancestor (*: $p<0.05$, **:
229 $p<0.01$, ***: $p<0.001$).

230

231 *Diversification involves mutations related to biofilm development, motility and metabolic pathways*

232 To get an idea of the genetic basis behind the observed diversification, genomes of selected SN (SN_A,
233 SN_E), SM (SM_D, SM_E) and WR (WR_A, WR_D and WR_E) isolates were re-sequenced. The genome
234 of the ancestor was previously re-sequenced (Dragoš *et al.,* 2018b), that revealed differences in the
235 genome sequence of our laboratory DK1042 stock compared to the database. In total, 43 non-
236 overlapping mutations (SNPs) were detected in the seven re-sequenced genomes, of which 38 were
237 single-nucleotide variants, 3 were deletions, and 2 were insertions (Table 1). Both SN_A and SN_E
238 harbored a single mutation, located in the gene coding for the biofilm master regulator, SinR. SM_D
239 and SM_E shared a mutation in the *flhB* gene, important for flagellar assembly, as well as numerous
240 mutations in the *gtaB* and *yvzE* genes, coding for UTP-glucose-1-phosphate uridylyltransferases. Each
241 of them harbored additional SNPs, a non-synonymous mutation in the glycerol facilitator coding gene,
242 *glpF*. Further, a synonymous mutation in *ydaD* gene was detected in SM_D, while SM_E additionally
243 carried non-synonymous mutations in the sporulation specific genes, *spoVR* and *dacB*. Finally, the
244 distinct WR isolates from different evolved populations shared no overlapping mutations, but
245 commonly harbored SNPs in genes related to motility (*fliI*, *fliR*, and *motB* in WR isolates from
246 population A, D, and E, respectively). WR_A and WR_D contained mutations in *pdeH* encoding a c-di-
247 GMP degrading phosphodiesterase, next to few additional mutations in these isolates. Because SM
248 isolates, evolved in independent populations, shared multiple identical mutations, genetic
249 heterogeneity might have already be present in the ancestral starting culture. Nonetheless, the rise
250 to detectable ratios of SM during the evolution indicates that they are advantageous for the
251 population and are, thus, selected for over time.

252

253 *Complementarity leads to enhanced productivity of mixed populations in root colonization*

254 Finally, we wondered how the SM isolates, which showed reduced pellicle biofilm development in
255 general and significantly reduced root colonization for one isolate, rose to and maintained low

256 frequencies throughout the evolution experiment and was not outcompeted over time during the
257 evolution. We hypothesized that its root colonization in the evolving populations might be facilitated
258 by other co-occurring morphotypes. Therefore, we tested the impact of diversity on individual and
259 group performance in root colonization by inoculating *A. thaliana* seedlings with SN, SM and WR in
260 monoculture as well as with a mix of all three morphotypes with equal starting frequencies (1:1:1) for
261 three different populations each (populations A, D, and E). We used an established method to
262 distinguish between selection, where variants that are most productive in monoculture tend to
263 dominate the mix, and complementarity, where most or all constituents tend to benefit from
264 biodiversity (Loreau & Hector, 2001; Poltak & Cooper, 2011).
265 Even though the mix of all three morphotypes tended to perform better in all three populations than
266 the ancestor (p_{PopA} = 0.0220, p_{PopD} = 0.0620, p_{PopE} = 0.0055), its CFU was the overall highest only in
267 population D, while in population A and E, it was lower than SN in monoculture, even though not
268 significantly (Fig. 5). However, the observed productivity of the three mixes were higher than their
269 respective predictions. To this end, a complementarity effect of biodiversity seemed to be the driving
270 force affecting the productivity of mixed populations. In population D, all three morphotypes
271 appeared to benefit from each other, as the CFU of each of the morphotypes were higher in the co-
272 culture than predicted, suggesting a mutualistic interaction. Productivity of SN increased thereby by
273 1.96-fold, SM by 2.50-fold and WR by 4.50-fold relative to their predicted CFU in the mix, resulting in
274 103% complementarity and -3% selection. On the contrary, in population A and E only SM and WR
275 benefited from the co-culture, while SN showed highly reduced CFU in the mix compared to its
276 prediction. In populations A and E, productivity of SN decreased by 0.18-fold and 0.47-fold, while it
277 increased for SM by 2.50-fold and 1.70-fold and WR by 20.72-fold and 4.75-fold, leading to 641% and
278 375% complementarity as well as -541% and -275% selection, respectively.

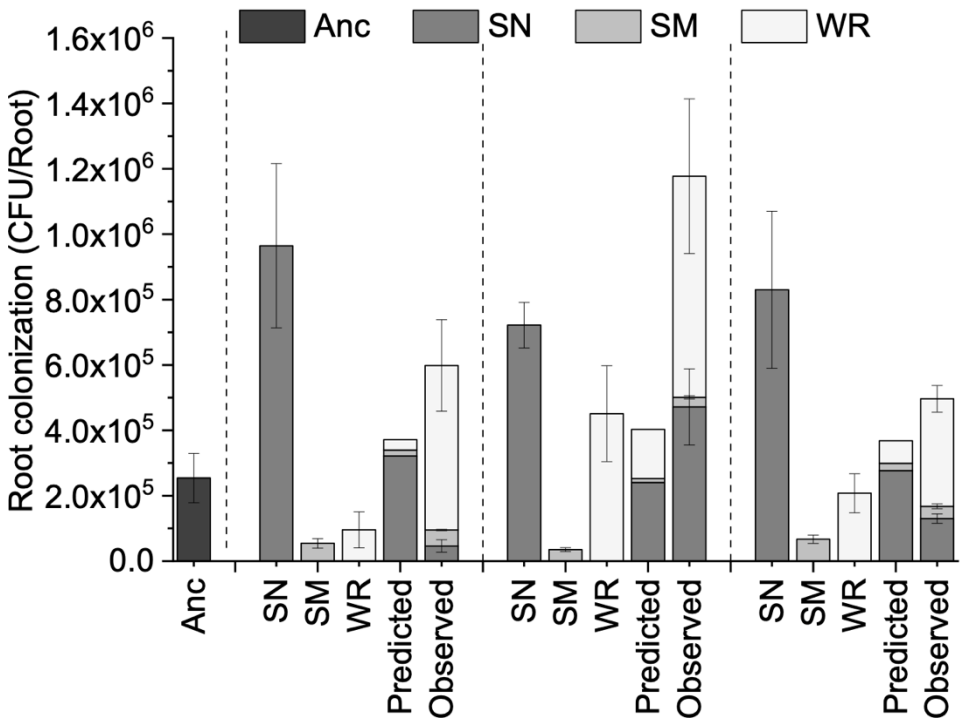

Fig. 5. Root colonization of morphotypes in monoculture as well as in a 1:1:1 mix or the ancestor. 14-16d old *A. thaliana* seedlings were inoculated with either the mix or the strains in monoculture and incubated for 48h in a plant chamber. The biofilm on the roots was disrupted by vortexing with small glass beads and the suspension was plated on solidified LB medium to allow CFU counting. Predicted colonization was calculated as the product of the proportion of each morphotype in the inoculum (1/3) and its performance (CFU per root) in monoculture. Observed colonization is the total colonization of the mixed community in the experimental setup. Bars represent the mean and error bars represent standard error for four replicates (9 replicates for ancestor pooled from different days).

289 **Discussion**

290 The PGPR *B. subtilis* is a promising sustainable alternative to traditionally used agrochemicals, as it
291 harbors many important plant growth-promoting and biocontrol properties while having reduced
292 negative effects on biodiversity and the environment (Blake *et al.,* 2021; Arnaouteli *et al.,* 2021). Even
293 though its potential seems immense under laboratory conditions and in greenhouse trials, the success
294 varies greatly when applied in fields (Peng *et al.,* 2011; Bardin *et al.,* 2015; Moreira & de Mio, 2015;
295 Wei *et al.,* 2016). To improve the application of *B. subtilis* within agriculture, we need a deeper
296 understanding of the underlying mechanisms of how it interacts with and colonizes plants. In this
297 work, we used experimental evolution to analyze how *B. subtilis* evolves on *A. thaliana* roots, by
298 continuously transferring a previously colonized root to a 100ml reagent bottle containing fresh
299 medium and a sterile root, thereby allowing only root-colonizing cells to be carried on throughout the
300 experiment. In contrast to the experimental evolution study by Batstone *et al.* (2020) that similarly
301 examined plant-microbe interaction, we focused solely on initial and re-colonization of plant roots by
302 *B. subtilis* in liquid minimal media with small plant seedlings. By using MSNg, a minimal media with
303 low glycerol concentrations that is insufficient to support growth and biofilm development of a *B.*
304 *subtilis* monoculture (Beauregard *et al.,* 2013), we promote bacteria being dependent on carbon
305 provided by the plant and possibly also being stimulated to move towards the root. Thus, by passaging
306 only the seedlings, and therefore only cells that attach tightly to the roots, we were able to select for
307 root colonization. Because traits such as motility, biofilm formation and dispersal as well as the
308 recognition and utilization of plant polysaccharides are assumed to be important and beneficial for
309 root (re-)colonization in our experimental set-up, we expected cells to improve in these properties
310 over time (Chen *et al.,* 2013; Allard-Massicotte *et al.,* 2016; Dragoš *et al.*, 2018a). Indeed, we observed
311 that *B. subtilis* populations rapidly increased in root colonization during the experimental evolution,
312 indicating fast adaptation to plant roots. In order to test whether genetic adaptation had taken place,
313 single evolved isolates from the final transfer (T20) were randomly selected for further
314 characterization, including growth and biofilm formation in response to plant polysaccharides.

315 Intriguingly, when testing evolved isolates from the final transfer for improved root colonization of *A.*
316 *thaliana* and tomato seedlings, we only observed improvements on *A. thaliana* indicating *A. thaliana*-
317 specific adaptation paths. Furthermore, we observed that evolving populations quickly diversified into
318 three distinct morphotypes, comprising a hyper-wrinkled SN variant, a round and smooth SM variant,
319 and a variant identical in colony morphology to the ancestor, termed WR. Finally, mixed colonization
320 of distinct morphotypes revealed a complementarity effect of biodiversity during root colonization, as
321 the performance of the mix exceeded the prediction based on individual performance of its
322 constituents (Fig. 5). Depending on the evolved population they originated from, SN, SM and WR
323 interacted either in a mutualistic way, as all three morphotypes benefited, or SM and WR most likely
324 exploited SN by capitalizing on overproduced matrix components.
325 Previous work proved that rapid diversification is commonly observed in microbial evolution and also
326 occurs in experimental evolution of *B. subtilis* in liquid LB culture under static and shaken conditions
327 as well as in biofilms (Leiman *et al.*, 2014; Dragoš *et al.,* 2018b; Richter *et al.,* 2018). Here, we
328 demonstrated that diversification of *B. subtilis* also plays an important role in experimental evolution
329 during ecologically- and biotechnologically-relevant plant root colonization. Diversification of *B.*
330 *subtilis* during evolution on *A. thaliana* roots seems highly reproducible, as the same evolutionary
331 pattern and highly similar morphotype frequencies could be observed in the final transfer of all five
332 parallel lines. The most striking difference between distinct morphotypes occurred in the complexity
333 in colony and pellicle architecture, indicating alterations in the capability of biofilm formation. In
334 addition to the hyper-wrinkled SN variant, from which all tested isolates showed hyper-robust biofilm
335 formation in the form of complex colonies and thick pellicles, a SM morphotype emerged that
336 seemingly had lost its ability to form a stable pellicle when inoculated solitarily. In accordance with
337 previous work by Chen *et al.* (2013), who tested correlation of pellicle formation with root colonization
338 of distinct natural isolates of *B. subtilis*, the evolved isolates displaying a more robust pellicle
339 formation, namely SN, also improved in root colonization. On the contrary, only one of the tested SM
340 isolates showed reduced root colonization, while unexpectedly the other SM isolate performed similar

341 to the ancestor on plant roots. Notably, dissimilar traits of the analogous morphotypes could be either
342 caused by additional mutations or alternatively, distinct mutations led to similar morphological, but
343 slightly different plant colonization consequences (Poltak & Cooper, 2011).
344 Remarkably, evolved isolates showed improvements in root colonization only on *A. thaliana*, but not
345 on tomato. In nature, the plant host species tend to be important drivers for diversity of the plant
346 microbiome, indicating active selection by the plant (Compant *et al.,* 2019). Furthermore, PGPR have
347 been shown to respond species-specifically in chemotaxis towards their original host plant where
348 these were isolated from (Zhang *et al.,* 2014). Distinct plant species produce and secrete distinct arrays
349 of root exudates, which act not only as a major carbon source for PGPR, but also as chemical signals
350 for bacterial chemotaxis and are, thus, important initiators of root colonization (Warembourg *et al.,*
351 2003; Beauregard, 2015). Similar to root exudates, the composition of plant polysaccharides, which
352 are known inducers of biofilm formation, differs between plant species (Beauregard *et al.,* 2013).
353 Lastly, the sheer differences in the physiological architecture of plant roots, including size, thickness,
354 abundance of lateral roots and root hairs, might provide even more variation in environmental
355 conditions between distinct plant species, thereby allowing plant species-specific adaptations (Saleem
356 *et al.,* 2018). Although the Arabidopsis-specific aspects of the adaptation mechanism still need to be
357 revealed, the evolved isolates performed differently on the two plant species.
358 Even though this report focuses mainly on phenotypical aspects of evolution of *B. subtilis* on *A.*
359 *thaliana* roots, we aimed to get a first impression of the genetic basis behind the adaptive
360 mechanisms, and consequently re-sequenced genomes of seven evolved isolates. In both of the tested
361 SN isolates, a mutation in the gene encoding the biofilm regulator SinR (A85T) was found. An identical
362 mutation in the *sinR* gene was previously observed resulting in hyper-wrinkled colony morphology,
363 increased expression of biofilm-related genes and enhanced matrix production (Chai *et al.,* 2010;
364 Leiman et al., 2014; Richter *et al.,* 2018; Kampf *et al.,* 2018). Intriguingly, both Richter *et al.* (2018) and
365 Kampf *et al.* (2018), observed spontaneous evolution of the exact same point mutation A85T in *sinR*,
366 indicating strong positive selection. Further, *ΔsinR* mutant *B. subtilis* with hyper-robust biofilm

367 displayed increased number of cells attached to plant roots (Chen *et al.,* 2013). These previously
368 reported data indicate that the observed mutation in *sinR* results in enhanced matrix production,
369 biofilm formation. Ultimately, enhanced biofilm matrix production resulted in increased root
370 colonization of the SN isolates. Unfortunately, observed mutations in SM and WR isolates are not as
371 self-explanatory as in SN, and, thus, we can only speculate about their consequences requiring further
372 molecular validation. The sequenced SM isolates harbored multiple mutations in *gtaB* and *yvzE* genes,
373 coding for UTP-glucose-1-phosphate uridylyltransferases synthesizing a precursor for
374 exopolysaccharide biosynthesis (Varon *et al.*, 1993). Intriguingly, acetylation of GtaB was
375 demonstrated to be important for proper biofilm formation in *B. subtilis* and a *gtaB* deletion mutant
376 showed reduced pellicle development (Reverdy *et al.,* 2018), suggesting that *gtaB* mutations could be
377 relevant in the observed SM morphotypes. In addition, we speculate that the multiple mutations in
378 *gtaB* possibly resulting in an unfunctional protein could explain the increased growth of the SM
379 isolates due to decreased EPS production. Two of the three WR variants carried distinct mutations in
380 the *pdeH* gene that encodes a c-di-GMP degrading phosphodiesterase, and additional, again distinct,
381 mutations in the intergenic region upstream of *ydaJ* that encodes a lipoprotein that may modify the
382 extracellular polysaccharide synthesized by YdaLMN proteins (Bedrunka & Graumann 2017). Notably,
383 perturbation of these genes slightly alters colony morphologies (Bedrunka & Graumann 2017). Finally,
384 all SM and WR morphotypes carried mutations in genes related to motility. While motility is not
385 essential for biofilm formation, motile strains are benefited in biofilm development compared to non-
386 motile derivates (Hölscher *et al.,* 2015), therefore these mutations might additionally impact the
387 efficiency of plant colonization. Nevertheless, overexpression of the *eps* operon in the SN
388 morphotypes due to *sinR* mutation, could also possibly impact motility due to the EpsE clutch (Blair *et*
389 *al.,* 2008). However, the role and impact of motility on the evolution of *B. subtilis* during plant root
390 colonization will be examined in future studies.
391 The observations and results from monoculture experiments are not able to explain how and why SM
392 variants, diminished in their ability to form biofilms and partially reduced in root colonization, are able

393 to arise and persist in populations during the evolution. Hence, we expected SM to capitalize on the
394 presence of other co-occurrent morphotypes. A general observation from several experimental
395 evolution studies with biofilm models is that the productivity of evolved populations not necessarily
396 equals to the sum of productivities of its members in monocultures, as interactions between distinct
397 evolved variants might occur (Brockhurst *et al.,* 2006; Poltak & Cooper, 2011; Ellis *et al.*, 2015). Overall,
398 biodiversity has been regarded to impact productivity of a community, by two distinct processes,
399 namely selection and complementarity (Loreau & Hector, 2001). Selective processes are anticipated
400 to lead to dominance of community members, which perform best in monoculture, as they are
401 expected to be able to outcompete others (Loreau & Hector, 2001). Complementary processes
402 comprise advantageous effects of biodiversity, where most or all constituents benefit (Loreau &
403 Hector, 2001). Interactions in a mixed community might, therefore, not always be positive, but can be
404 also negative, as either mutualistic interactions, e.g. cross-feeding and niche construction, or
405 antagonistic interactions, e.g. cheats and exploitation, might evolve (Day & Young, 2004; Poltak &
406 Cooper, 2011, Dragoš *et al.,* 2018b). Here, we extend these observations with a biotechnological
407 relevant system on plant roots, describing the evolution of both exploitative as well as mutualistic
408 interactions between the evolved morphotypes in distinct evolutionary lineages. The number of cells
409 colonizing plant roots with an initially equal mix of SN, SM and WR is higher compared to its prediction
410 in all three tested evolutionary lineages. Indeed, a complementarity effect of biodiversity seemed to
411 be the cause for this "overyielding" of the mixed community. However, only in one of the three tested
412 populations, namely in the mix of population D, all three morphotypes seemed to benefit from being
413 in this mix, indicating mutualistic interactions. Further, this was the only tested population, were the
414 mix outperformed all monocultures. In the other two tested evolved populations, even though the
415 mix performed better than the ancestor, the three members population did not outperform the best
416 performing monoculture, namely SN. Additionally, SN showed strongly reduced CFU in these two
417 mixes compared to its predicted value, suggesting that only WR and SM benefited. The observed
418 mutation in *sinR* in SN suggests that it overproduces matrix components, a public good that is costly,

419 but can be capitalized on. We speculate that WR and SM possibly exploit this, by integrating into the
420 matrix without having the cost of its production, improving their own productivity in mixed
421 colonization at the expense of SN. Considering that SM was observed during experimental evolution
422 only after SN rose to detectable levels in each of the five parallel populations, it is reasonable to infer
423 that SM is able to arise and persist in evolved populations by capitalizing on the enhanced matrix
424 provided by SN. Similar to our study, Dragoš *et al.* (2018b) observed the evolution of a non-producing
425 and matrix-exploiting smooth morphotype in *B. subtilis* pellicles. The described smooth variant
426 integrated and resided in the biofilm produced by co-occurring morphotypes, thus, exploiting matrix
427 production (Dragoš *et al.,* 2018b).
428 Even more significantly, complementary effects are observed during root colonization by distinct
429 morphotypes, evolved from a shared ancestor, in all tested populations. Indeed, a negative selection
430 effect of biodiversity, as observed for all three populations here, indicates that the best root colonizing
431 variant in monoculture is losing out in a mixed community. This requires attention in future studies,
432 as it raises many questions about the influence of the natural diversity in the rhizosphere on the
433 application of *B. subtilis*. Further, the observation that interactions between the three morphotypes
434 differed in distinct evolved populations indicates that biodiversity both evolved and is maintained
435 differently in the parallel populations (Poltak & Cooper, 2011). Nevertheless, further experiments are
436 needed to reveal whether similar ecological interactions exist among the isolates from distinct
437 lineages.
438 In conclusion, our results suggest that *B. subtilis* adapts rapidly to root colonization on *A. thaliana.* Our
439 findings are relevant for the application of *B. subtilis* as a PGPR in agriculture, as they imply that genetic
440 diversification might be a stable strategy for root colonization, and a mix of distinct phenotypic
441 variants might be more beneficial compared to one single strong root colonizer. In addition to a
442 potential increase in net productivity on plant roots, a diverse mix might be more resistant to invasions
443 by non-cooperating cheaters (Brockhurst *et al.,* 2006), therefore, enhancing also the maintenance of
444 the biofilm formed on the root.

445 **Experimental procedures**

446 *Bacterial strains and culture conditions*

447 Throughout this study, the ancestral strain *B. subtilis* DK1042 (natural competent variant of the
448 undomesticated NCIB 3610 (Konkol *et al.,* 2013)) and evolved derivatives were grown in Lysogeny
449 Broth (LB) (Lennox, 10 $g \cdot l^{-1}$ Tryptone, 5 $g \cdot l^{-1}$ Yeast Extract and 5 $g \cdot l^{-1}$ NaCl) over night (ON) at 37°C. For
450 formation of complex colonies, 2µl of exponential phase culture were spotted on LB medium solidified
451 with 1.5% agar and incubated at 30°C for 48h. To assay pellicle formation, the OD_{600} of a bacterial
452 culture in exponential phase was adjusted to 5, and 15µl were inoculated into 1ml of LB + 0.5% xylan
453 (from beechwood, Carl Roth) in 24-well microtiter plates and incubated at 30°C for 48h. In order to
454 analyze growth in response to plant polysaccharides, the OD_{600} of a bacterial culture in exponential
455 phase was adjusted to 0.1 in a minimal salt medium (MSN) (5mM potassium phosphate buffer pH 7.0,
456 0.1M 3-(N-morpholino)propanesulfonic acid pH 7.0, 4 $mmol \cdot l^{-1}$ $MgCl_2$, 0.05 $mmol \cdot l^{-1}$ $MnCl_2$, 1 $\mu mol \cdot l^{-1}$
457 $ZnCl_2$, 2 $\mu mol \cdot l^{-1}$ thiamine, 700 $\mu mol \cdot l^{-1}$ $CaCl_2$, 0.2 % NH_4Cl) supplemented with 0.5% cellobiose (Carl
458 Roth) (MSNc) and 0.5% xylan, because xylan and cellulose have been previously observed to support
459 growth of *B. subtilis* (Beauregard *et al.*, 2013). 100µl was transferred to a 96-well plate and incubated
460 in a plate reader (BioTek Synergy HTX Multi-Mode Microplate Reader) for 58h at 24°C, orbital shaking.
461 OD_{600} was measured every 15 minutes in a 9-point measurement at different points of each well, to
462 exclude errors of clumping and inhomogeneous suspensions. Afterwards, each well was analyzed
463 under the stereomicroscope to confirm no visible aggregation or pellicles formed, which would skew
464 OD_{600} measurements. Exponential phase of growth curves was identified with a linear regression
465 model and growth rates (r) were calculated. For root colonization experiments MSN supplemented
466 with 0.05% glycerol (MSNg) was used.

467

468 *Seedling preparation*

469 In this study, both *A. thaliana* ecotype Col-0 and tomato (*Solanum lycopersicum L.*, Maja Buschtomato,
470 Buzzy Seeds, NL) seedlings were used. Seeds were surface sterilized in Eppendorf tubes by shaking

471 vigorously with an orbital mixer for 12 minutes in 1mL 2% sodium hypochlorite. Afterwards, seeds
472 were washed five times in 1 ml sterile MiliQ water through alternating centrifugation and removal of
473 liquid solution. After sterilization, 8-10 seeds were plated on pre-dried 1% MS-agar (Murashige and
474 Skoog basal salts mixture; Sigma) (2.2 g l^{-1}) ensuring that the seedlings have sufficient space for proper
475 root development and plates were sealed with parafilm. *A. thaliana* seeds were stratified in the dark
476 at 4°C for 2-3d and subsequently incubated in a plant chamber with a day/night cycle of 16h light at
477 24°C and 8h dark at 20°C for 12-14d at an angle of 65°. Tomato seeds were moved to the plant
478 chamber without stratification and incubated for 6-8d.
479
480 *Experimental evolution*
481 We established an experimental evolution approach inspired by the bead transfer model of Poltak &
482 Cooper (2011) to study *B. subtilis* evolution on plant roots, similar to the setup exploited for *Bacillus*
483 *thuringiensis* (Lin *et al.,* 2020). Therefore, every other day, a previously colonized plant seedling was
484 transferred to a new sterile seedling, allowing only bacterial cells that attach to the new root to
485 continue in the experiment, enabling selection for a continuous cycle of dispersal, chemotaxis towards
486 the plant root, and biofilm formation on the root. To start the experimental evolution, five 14-16d old
487 *A. thaliana* Col-0 seedlings (population A to E) were placed in 100mL reagent bottles containing 27ml
488 of MSNg, and inoculated with 3ml of bacterial culture of *B. subtilis* DK1042 adjusted to OD_{600} of 0.2,
489 reaching a starting OD_{600} of 0.02. To ensure that only the roots but not sprout or leaves provided
490 surface for colonization, the seedlings were pulled through a sterile nylon mesh floating on top of the
491 liquid medium, leaving only the roots submerged in the medium (Harris *et al.,* 2019). Seedlings were
492 incubated for 48 hours under static conditions in a plant chamber with a day/night cycle of 16h light
493 at 24°C and 8h dark at 20°C. Before the transfer, the mesh of the previously colonized root was
494 removed and the seedling was carefully washed in sterile MilliQ water, in order to remove non-
495 colonizing cells. Subsequently, the colonized seedling was placed in fresh medium containing a new
496 sterile seedling, allowing re-colonization. Evolving populations were continuously passaged every 48h

497 for a total of 40 days (20 subsequently colonized seedlings per population). In order to keep track and
498 ensure sterile handling of seedlings during the evolution, two controls without initial inoculant were
499 included, in which either sterile seedlings or 10% of the MSNg medium were passaged. To follow the
500 development of the populations and test for contamination, the bacterial cells colonizing the old
501 roots, as well as the two controls, were plated on LB agar medium after initial colonization and transfer
502 5, 10, 17 and 20. In order to disperse the biofilm from the seedling for the quantification, roots were
503 detached from the sprout, carefully washed in sterile MilliQ, and vortexed vigorously for 3 minutes in
504 1ml of 0.9% NaCl with small glass beads (Glass beads Ø0.75-1.00 mm, Carl Roth). The resulting cell
505 suspensions were plated for CFU quantification and saved as frozen stocks for later comparison.
506
507 *Morphological diversification*
508 Distinct morphotypes of evolved populations were determined according to characteristics in colony
509 morphology (shape, size and color) on LB agar medium. To ensure different morphotypes were
510 genetically stable, three random colonies of each variant were isolated and passaged every 24h for
511 three transfers either in liquid LB, on LB agar medium as well as alternating between the two media
512 for four transfers. After the final transfer, cultures were serial diluted and plated on LB-Agar to assess
513 colony morphology. In order to analyze the development of the ratio of each morphotype during the
514 evolution, a bacterial culture prepared from the frozen stock of each population for transfer 5, 10, 17,
515 and 20, as well as of the ancestor as starting point 0, was grown to log-phase, diluted, plated on LB-
516 agar in triplicates for two dilutions and incubated for 16h at 30°C. Subsequently, morphotypes were
517 identified, all colonies were counted, with a minimum of 50 and an average of 100 colonies per plate,
518 and ratios were calculated (Leiman *et al.*, 2014).
519
520 *Root colonization productivity*
521 In order to analyze whether evolved isolates were improved in root colonization compared to the
522 ancestor, and whether those improvements were specific for the plant species the isolates evolved

523 on, root colonization was tested on both *A. thaliana* Col-0 and tomato seedlings. Therefore, three
524 single isolates were picked randomly from the final populations (i.e. T20) of linages A, C, D, and E. 14-
525 16d old *A. thaliana* and 6-8d old tomato seedlings were inoculated with each of the evolved isolates
526 in four replicates as described previously for initiation of the experimental evolution. After
527 confirmation of equal variance with Levene´s test and normality of data with Shapiro–Wilk test,
528 changes in root colonization were analyzed for significance with Dunnett´s post hoc test. Furthermore,
529 to test the impact of diversity on the individual and mixed performance in root colonization, 14-16d
530 old *A. thaliana* seedlings were inoculated with a 1:1:1 mix of pre-grown cultures of the three distinct
531 morphotypes (SN, SM and WR), originating from the same evolved population (population A, D and
532 E). Random colonies of each of the three morphotypes have been newly isolated for population A and
533 D, because one of the morphotypes lacked in either population. Further, this ensured avoidance of a
534 potential bias from previous monoculture experiments caused by different performances of the two
535 tested WR isolates, e.g. WR_A and WR_Ab, in each of the populations. For population E, previously
536 tested SN_E, SM_E and WR_E were used. Seedlings were incubated together with the bacterial
537 inoculant for 48h in the plant chamber to allow root colonization. Afterwards, seedlings were carefully
538 washed in sterile MilliQ water, the biofilm formed on plant roots was disrupted and the bacterial
539 suspensions were plated on LB agar medium to allow CFU quantification. For mixed colonization, the
540 predicted root colonization was calculated by multiplying the root colonization of each constituent in
541 mono culture with the ratio in the inoculum (1/3) (Loreau & Hector, 2001; Poltak & Cooper, 2011).
542 Further, selection and complementarity effect have been calculated as described by Loreau & Hector
543 (2001).
544
545 *Microscopy*
546 Bright field images of whole pellicles and colonies were obtained with an Axio Zoom V16
547 stereomicroscope (Carl Zeiss, Germany) equipped with a Zeiss CL 9000 LED light source and an
548 AxioCam MRm monochrome camera (Carl Zeiss, Germany).

549

550 *Statistical analysis*

551 At least three replicates were conducted for all experiments. Statistical analysis was performed in R
552 4.0.3. In detail, Shapiro-Wilk test and Levene's test were performed to test for normality and equality
553 of variance, respectively. To test for outlier, Grubb´s tests were conducted. For comparison between
554 ancestor and evolved isolates, as well as between the first and following transfers during experimental
555 evolution, ordinary one-way ANOVA analysis corrected with Benjamini-Hochberg procedure and
556 Dunnett´s tests were employed. In order to test for significance in differences between predicted and
557 observed CFU on roots in mixed colonization, Student´s t-tests were performed.

558

559 *Genome resequencing and genome analysis*

560 Resequencing of evolved isolates was performed as previously (Dragoš *et al.,* 2018b; Dragoš *et al.,*
561 2018c; Martin *et al.,* 2020; Thérien *et al.,* 2020; Gallegos-Monterrosa *et al.,* 2021). Genomic DNA of
562 selected evolved isolates from the final transfer was extracted from 2ml ON cultures using the EURx
563 Bacterial and Yeast Genomic DNA Kit. Paired-end libraries were prepared using the NEBNext® Ultra™
564 II DNA Library Prep Kit for Illumina. Paired-end fragment reads were generated on an Illumina NextSeq
565 sequencer using TG NextSeq® 500/550 High Output Kit v2 (300 cycles). Primary data analysis (base-
566 calling) was carried out with "bcl2fastq" software (v2.17.1.14, Illumina). All further analysis steps were
567 done in CLC Genomics Workbench Tool 9.5.1. Reads were quality-trimmed using an error probability
568 of 0.05 (Q13) as the threshold. In addition, the first ten bases of each read were removed. Reads that
569 displayed ≥80% similarity to the reference over ≥80% of their read lengths were used in the mapping.
570 Non-specific reads were randomly placed to one of their possible genomic locations. Quality-based
571 SNP and small In/Del variant calling was carried out requiring ≥8 × read coverage with ≥25% variant
572 frequency. Only variants supported by good quality bases (Q ≥ 20) were considered and only when
573 they were supported by evidence from both DNA strands in comparison to the *B. subtilis* NCIB 3610
574 genome and pBS plasmid (GenBank accession no. NZ_CP020102 and NZ_CP020103, respectively).

575 Identified mutations in each strain are listed in Table 1. Raw sequencing data has been deposited to

576 the NCBI Sequence Read Archive (SRA) database under BioProject accession number: PRJNA705297

577

578 **Conflict of interests**

579 The authors declare that there is no conflict of interests in relation to the work described.

580 **References**

581 Allard-Massicotte, R., Tessier, L., Lécuyer, F., Lakshmanan, V., Lucier, J. F., Garneau, D., *et al.* (2016)
582 *Bacillus subtilis* early colonization of *Arabidopsis thaliana* roots involves multiple chemotaxis
583 receptors. *mBio* **7:** e01664-16.

584 Arkhipova, T.N., Veselov, S U., Melentiev, A.I., Martynenko, E.V., and Kudoyarova, G.R. (2005) Ability
585 of bacterium *Bacillus subtilis* to produce cytokinins and to influence the growth and endogenous
586 hormone content of lettuce plants. *Plant Soil* **272:** 201-209.

587 Arnaouteli, S., Bamford, N., Stanley-Wall, N., and Kovács, Á.T. (2021) *Bacillus subtilis* biofilm formation
588 and social interactions. *Nat Rev Microbiol* https://doi.org/10.1038/s41579-021-00540-9

589 Bardin, M., Ajouz, S., Comby, M., Lopez-Ferber, M., Graillot, B., Siegwart, M., and Nicot, P.C. (2015) Is
590 the efficacy of biological control against plant diseases likely to be more durable than that of chemical
591 pesticides? *Front Plant Sci* **6:** 566.

592 Batstone, R T., O'Brien, A.M., Harrison, T.L., and Frederickson, M.E. (2020) Experimental evolution
593 makes microbes more cooperative with their local host genotype. *Science* **370:** 476-478.

594 Beauregard, P. B. Chai, Y. Vlamakis, H. Losick, R. and Kolter, R. (2013) *Bacillus subtilis* biofilm induction
595 by plant polysaccharides. *Proc Natl Acad Sci U S A* **110:** E1621-E1630.

596 Beauregard, P. B. (2015) Not just sweet talkers: How roots stimulate their colonization by beneficial
597 bacteria. *Adv Bot Res* **75:** 1-20.

598 Bedrunka, P., and Graumann, P.L. (2017) Subcellular clustering of a putative c-di-GMP-dependent
599 exopolysaccharide machinery affecting macro colony architecture in *Bacillus subtilis*. *Environ*
600 *Microbiol Rep* **9:** 211-222.

601 Blair, K.M., Turner, L., Winkelman, J.T., Berg, H.C., and Kearns, D.B. (2008) A molecular clutch disables
602 flagella in the *Bacillus subtilis* biofilm. *Science* **320:** 1636-1638.

603 Blake, C., Christensen, M.N., and Kovács, Á.T. (2021) Molecular aspects of plant growth promotion and
604 protection by *Bacillus subtilis*. *Mol Plant Microbe Interact* **34:** 15-25.

605 Branda, S.S., Chu, F., Kearns, D B., Losick, R., and Kolter, R. (2006) A major protein component of the
606 *Bacillus subtilis* biofilm matrix. *Mol Microbiol* **59:** 1229-1238.
607 Brockhurst, M.A., Hochberg, M.E., Bell, T., and Buckling, A. (2006) Character displacement promotes
608 cooperation in bacterial biofilms. *Curr Biol* **16:** 2030-2034.
609 Cazorla, F.M., Romero, D., Pérez-García, A., Lugtenberg, B.J.J., Vicente, A.D., and Bloemberg, G. (2007)
610 Isolation and characterization of antagonistic *Bacillus subtilis* strains from the avocado rhizoplane
611 displaying biocontrol activity. *J Appl Microbiol* **103:** 1950-1959.
612 Chai, Y., Norman, T., Kolter, R., and Losick, R. (2010) An epigenetic switch governing daughter cell
613 separation in *Bacillus subtilis*. *Genes Dev* **24:** 754-765.
614 Chen, Y., Yan, F., Chai, Y., Liu, H., Kolter, R., Losick, R., and Guo, J.H. (2013) Biocontrol of tomato wilt
615 disease by *Bacillus subtilis* isolates from natural environments depends on conserved genes mediating
616 biofilm formation. *Environ Microbiol* **15:** 848-864.
617 Compant, S., Samad, A., Faist, H., and Sessitsch, A. (2019) A review on the plant microbiome: ecology,
618 functions, and emerging trends in microbial application. *J Adv Res* **19:** 29-37.
619 Day, T., and Young, K.A. (2004) Competitive and facilitative evolutionary diversification. *BioScience* **54:**
620 101-109.
621 Deng, Y., Chen, H., Li, C., Xu, J., Qi, Q., Xu, Y., et al. (2019) Endophyte *Bacillus subtilis* evade plant
622 defense by producing lantibiotic subtilomycin to mask self-produced flagellin. *Commun Biol* **2:** 368.
623 Dragoš, A., Kiesewalter, H., Martin, M., Hsu, C.Y., Hartmann, R., Wechsler, T., *et al.* (2018a) Division of
624 labor during biofilm matrix production. *Curr Biol* **28:** 1903-1913.
625 Dragoš, A., Lakshmanan, N., Martin, M., Horváth, B., Maróti, G., Falcón García, C., Lieleg, O., and
626 Kovács, Á.T. (2018b) Evolution of exploitative interactions during diversification in *Bacillus subtilis*
627 biofilms. *FEMS Microbiol Ecol* **94:** fix155
628 Dragoš, A., Martin, M., Falcón García, C., Kricks, L., Pausch, P., Heimerl, T., *et al.* (2018c) Collapse of
629 genetic division of labor and evolution of autonomy in pellicle biofilms. *Nat Microbiol* **3:** 1451-1460

630 Ellis, C.N., Traverse, C.C., Mayo-Smith, L., Buskirk, S.W., and Cooper, V.S. (2015) Character
631 displacement and the evolution of niche complementarity in a model biofilm community. *Evol* **69:** 283-
632 293.
633 Fitzpatrick, C.R., Copeland, J., Wang, P. W., Guttman, D.S., Kotanen, P.M., and Johnson, M.T. (2018)
634 Assembly and ecological function of the root microbiome across angiosperm plant species. *Proc Natl*
635 *Acad Sci U S A* **115:** E1157-E1165.
636 Gallegos-Monterrosa, R., Christensen, M.N., Barchewitz, T., Köppenhöfer, S., Priyadarshini, B., Bálint,
637 B., *et al.* (2021) Impact of Rap-Phr system abundance on adaptation of *Bacillus subtilis*. *Commun Biol*
638 **4:** 468.
639 Harris, S.L., Pelaez, C.A., and Shank, E.A. (2019) Monitoring bacterial colonization and maintenance on
640 *Arabidopsis thaliana* roots in a floating hydroponic system. *J Vis Exp* **147:** e59517.
641 Hölscher, T., Bartels, B., Lin, Y. C., Gallegos-Monterrosa, R., Price-Whelan, A., Kolter, R., *et al.* (2015)
642 Motility, chemotaxis and aerotaxis contribute to competitiveness during bacterial pellicle biofilm
643 development. *J Mol Biol* **427:** 3695-3708.
644 Kampf, J., Gerwig, J., Kruse, K., Cleverley, R., Dormeyer, M., Grünberger, A., *et al.* (2018) Selective
645 pressure for biofilm formation in *Bacillus subtilis*: differential effect of mutations in the master
646 regulator SinR on bistability. *mBio* **9:** e01464-18.
647 Kawecki, T.J., Lenski, R.E., Ebert, D., Hollis, B., Olivieri, I., and Whitlock, M.C. (2012) Experimental
648 evolution. *Trends Ecol Evol* **27:** 547-560.
649 Konkol, M.A., Blair, K.M., and Kearns, D.B. (2013) Plasmid-encoded ComI inhibits competence in the
650 ancestral 3610 strain of *Bacillus subtilis*. *J Bacteriol* **195:** 4085-4093.
651 Leiman, S. A., Arboleda, L. C., Spina, J. S., and McLoon, A. L. (2014) SinR is a mutational target for fine-
652 tuning biofilm formation in laboratory-evolved strains of *Bacillus subtilis*. *BMC Microbiol* **14:** 301.
653 Lin, Y., Alstrup, M., Pang, J.K.Y., Maróti, G., Er-Rafik, M., Tourasse, N., *et al.* (2020) Adaptation of
654 *Bacillus thuringiensis* to plant colonisation affects differentiation and toxicity. *bioRxiv*
655 https://doi.org/10.1101/2020.12.03.410076

656 Loreau, M., and Hector, A. (2001) Partitioning selection and complementarity in biodiversity
657 experiments. *Nature* **412:** 72-76.
658 Lugtenberg, B., and Kamilova, F. (2009) Plant-growth-promoting rhizobacteria. *Annu Rev Microbiol* **63:**
659 541-556.
660 Luo, C., Zhou, H., Zou, J., Wang, X., Zhang, R., Xiang, Y., and Chen, Z. (2015) Bacillomycin L and surfactin
661 contribute synergistically to the phenotypic features of *Bacillus subtilis* 916 and the biocontrol of rice
662 sheath blight induced by *Rhizoctonia solani*. *Appl Microbiol Biotechnol* **99:** 1897-1910.
663 Martin, M., Dragoš, A., Otto, S.B., Schäfer, D., Brix, S., Maróti, G., and Kovács, Á.T. (2020) Cheater-
664 mediated evolution shifts phenotypic heterogeneity in *Bacillus subtilis* biofilms. *ISME J* **14:** 2302-2312.
665 Moreira, R. R., and De Mio, L. L. M. (2015) Potential biological agents isolated from apple fail to control
666 Glomerella leaf spot in the field. *Biol Control* **87:** 56-63.
667 McDonald, M.J. (2019) Microbial Experimental Evolution–a proving ground for evolutionary theory
668 and a tool for discovery. *EMBO Rep* **20:** e46992.
669 Micallef, S.A., Shiaris, M.P., and Colón-Carmona, A. (2009) Influence of *Arabidopsis thaliana* accessions
670 on rhizobacterial communities and natural variation in root exudates. *J Exp Bot* **60:** 1729-1742.
671 Nordgaard, M., Mortensen, R.M.R., Kirk, N.K., Gallegos-Monterrosa, R., and Kovács, Á.T. (2021)
672 Deletion of Rap-Phr systems in *Bacillus subtilis* influences *in vitro* biofilm formation and plant root
673 colonization. *Microbiol Open* **10:** e1212.
674 Peng, G., McGregor, L., Lahlali, R., Gossen, B.D., Hwang, S.F., Adhikari, K.K., Strelkov, S.E, and
675 McDonald, M.R. (2011) Potential biological control of clubroot on canola and crucifer vegetable crops.
676 *Plant Pathol* **60:** 566-574.
677 Pieterse, C.M., Zamioudis, C., Berendsen, R.L., Weller, D.M., Van Wees, S.C., and Bakker, P.A. (2014)
678 Induced systemic resistance by beneficial microbes. *Annu Rev Phytopath* **52:** 347-375.
679 Poltak, S.R., and Cooper, V.S. (2011) Ecological succession in long-term experimentally evolved
680 biofilms produces synergistic communities. *ISME J* **5:** 369-378.

681 Reverdy, A., Chen, Y., Hunter, E., Gozzi, K., and Chai, Y. (2018) Protein lysine acetylation plays a
682 regulatory role in *Bacillus subtilis* multicellularity. *PLoS One* **13:** e0204687.
683 Richter, A., Hölscher, T., Pausch, P., Sehrt, T., Brockhaus, F., Bange, G., and Kovács, Á.T. (2018)
684 Hampered motility promotes the evolution of wrinkly phenotype in *Bacillus subtilis*. *BMC Evol Biol* **18:**
685 155.
686 Saleem, M., Law, A.D., Sahib, M.R., Pervaiz, Z.H., and Zhang, Q. (2018) Impact of root system
687 architecture on rhizosphere and root microbiome. *Rhizosphere* **6:** 47-51.
688 Saravanakumar, D., Kavino, M., Raguchander, T., Subbian, P., and Samiyappan, R. (2011) Plant growth
689 promoting bacteria enhance water stress resistance in green gram plants. *Acta Physiol Plant* **33:** 203-
690 209.
691 Shoda, M. (2000) Bacterial control of plant diseases. *J Biosci Bioeng* **89:** 515-521.
692 Sivasakthi, S., Usharani, G., and Saranraj, P. (2014) Biocontrol potentiality of plant growth promoting
693 bacteria (PGPR)-*Pseudomonas fluorescens* and *Bacillus subtilis*: A review. *African J Agricult Res* **9:** 1265-
694 1277.
695 Thérien, M., Kiesewalter, H.T., Auria, E., Charron-Lamoureux, V., Wibowo, M., Maróti, G., *et al.* (2020)
696 Surfactin production is not essential for pellicle and root-associated biofilm development of *Bacillus*
697 *subtilis*. *Biofilm* **2:** 100021
698 Todorova, S., and Kozhuharova, L. (2010) Characteristics and antimicrobial activity of *Bacillus subtilis*
699 strains isolated from soil. *World J Microbiol Biotechnol* **26:** 1207-1216.
700 Trivedi, P., Leach, J.E., Tringe, S.G., Sa, T., and Singh, B.K. (2020) Plant–microbiome interactions: From
701 community assembly to plant health. *Nat Rev Microbiol* **18:** 607-621.
702 van Gestel, J., Weissing, F.J., Kuipers, O.P., and Kovács, Á.T. (2014) Density of founder cells affects
703 spatial pattern formation and cooperation in *Bacillus subtilis* biofilms. *ISME J* **8:** 2069-2079.
704 Vandenkoornhuyse, P., Quaiser, A., Duhamel, M., Le Van, A., and Dufresne, A. (2015) The importance
705 of the microbiome of the plant holobiont. *New Phytol* **206:** 1196-1206.

706 Varon, D., Boylan, S. A., Okamoto, K., and Price, C. W. (1993) *Bacillus subtilis gtaB* encodes UDP-
707 glucose pyrophosphorylase and is controlled by stationary-phase transcription factor sigma B. *J*
708 *Bacteriol* **175:** 3964-3971.
709 Warembourg, F.R., Roumet, C., and Lafont, F. (2003) Differences in rhizosphere carbon-partitioning
710 among plant species of different families. *Plant Soil* **256:** 347-357.
711 Wei, F., Hu, X., and Xu, X. (2016) Dispersal of *Bacillus subtilis* and its effect on strawberry phyllosphere
712 microbiota under open field and protection conditions. *Sci Rep* **6:** 22611.
713 Yi, H.S., Yang, J.W., Ghim, S.Y., and Ryu, C.M. (2011) A cry for help from leaf to root: Above ground
714 insect feeding leads to the recruitment of rhizosphere microbes for plant self-protection against
715 subsequent diverse attacks. *Plant Signal Behav* **6:** 1192-1194.
716 Zhang, N., Wang, D., Liu, Y., Li, S., Shen, Q., and Zhang, R. (2014) Effects of different plant root exudates
717 and their organic acid components on chemotaxis, biofilm formation and colonization by beneficial
718 rhizosphere-associated bacterial strains. *Plant Soil* **374:** 689-700.
719 Zhang, F., Kwan, A., Xu, A., and Süel, G.M. (2015) A synthetic quorum sensing system reveals a
720 potential private benefit for public good production in a biofilm. *PLoS One* **10:** e0132948.
721 Zhu, B., and Stülke, J. (2017) SubtiWiki in 2018: from genes and proteins to functional network
722 annotation of the model organism Bacillus subtilis. *Nucl Acids Res* **46:** D743-748
723

724 **Table 1.** List of mutations detected in the genomes of re-sequenced morphotypes. Functions of the

725 gene products were retrieved from SubtiWiki Database (Zhu & Stülke, 2017)

SN		SM		WR			Position	Gene	Mutation	Function of gene product
SN_A	SN_E	SM_D	SM_E	WR_A	WR_D	WR_E				
		✓					472036	*ydaD*	288G>T	general stress protein
				✓			478790	*intergenic*	C>G	upstream region of *ydaJ* that codes for a lipoprotein that may modify the extracellular polysaccharide synthesized by YdaLMN proteins
					✓		478876	*intergenic*	T>del	
		✓					1002770	*glpF*	Pro78Ala	glycerol facilitator
			✓				1016370	*spoVR*	Glu229Gly	spore cortex synthesis
				✓			1391100	*thiU*	Pro192Gln	thiamine uptake
						✓	1433817	*motB*	Gly226Asp	flagellar motor rotation
				✓			1696818	*fliI*	Thr304Lys	flagellar-specific ATPase
					✓		1706108	*fliR*	Ala89_Ala93del	part of the flagellar Type III secretion system
		✓	✓				1707666	*flhB*	Glu347fs	part of the flagellar Type III secretion system
			✓				2424537	*dacB*	Ala7Thr	sporulation-specific penicillin-binding protein
✓	✓						2552926	*sinR*	Ala85Thr	control of biofilm formation
				✓			2578188	*pstBA*	Ser216Pro	phosphate ABC transporter ATP-binding protein
					✓		3258864	*pdeH*	Asp137fs	degradation of c-di-GMP
				✓			3258936		Asp116Tyr	
		✓	✓				3666149	*gtaB*	483G>A	UTP-glucose-1-phosphate uridylyltransferase
		✓	✓				3666155		489G>A	
		✓	✓				3666161		Glu165Asp	
		✓	✓				3666171		Arg169Cys	
		✓	✓				3666173		507C>T	
		✓	✓				3666176		510C>T	
			✓				3666182		516T>C	
		✓	✓				3673066	*yvzE*	Phe27Val	putative UTP-glucose-1-phosphate uridylyltransferase
		✓	✓				3673068		Phe27Leu	
		✓	✓				3673077		90A>T	
		✓	✓				3673098		Asp37Glu	
		✓	✓				3673101		114A>T	

726